Crystallite Size and Lattice Strain Evolution in a Nanostructured 6063-T1 Aluminum Alloy Processed by Equal Channel Angular Pressing

NICOLAE SERBAN, DOINA RADUCANU, MIHAI BUTU*, VASILE DANUT COJOCARU
University Politehnica of Bucharest, Materials Science and Engineering Faculty, 313 Spl. Independenței, 060042, Bucharest, Romania

Equal Channel Angular Pressing (ECAP) is the most emblematic technique for producing bulk nanostructured materials and ultrafine grained materials (UFG) through severe plastic deformation. In this study, we examined a 6063-T1 aluminum alloy, subjected to ECAP processing at room temperature for one, three, six and nine passes respectively, using a 90° die and the processing route B_C. The as-received and ECAP processed samples were firstly analyzed in OES experiments, the accumulated equivalent strain being also estimated based on ECAP die geometry and on the number of passes. All specimens were investigated as well in XRD tests for phase identification. Williamson-Hall method was used for evaluating the crystallite size and the lattice strain. Some correlations with the main processing parameters were also established.

Keywords: XRD analysis, Williamson-Hall method, severe plastic deformation, equal channel angular pressing, nanostructured aluminum

Materials with submicrometer grain sizes were classified as ultrafine grained (UFG) materials, with grain sizes between 100 nm and 1000 nm and nanostructured materials (NM), having crystallite sizes smaller than 100 nm [1-3]. Structural characteristics of UFG and NM can be analyzed *via* X-Ray diffraction (XRD) technique, this analysis leading primarily to crystalline phases identification. XRD technique is also widely used for establishing the dimensional parameters of crystals, spacing between crystallographic planes, diffraction planes and lattice parameters. Nowadays, XRD analysis can be used for evaluation of both crystallite size and microstrain (nanocrystals) as well, as the Williamson-Hall technique, which is in fact Scherrer's equation corrected for considering also the lattice strain effect on diffraction peaks shape [4]:

$$FWHM \cdot \cos\theta = \frac{K \cdot \lambda}{D} + \varepsilon \cdot \sin\theta \qquad (1)$$

where:

FWHM is the full width at half maximum;
θ is the diffraction peak position from the XRD pattern;
K is the crystalline domain shape factor;
λ is the X-ray wavelength;
D is the crystallite size and ε is the microstrain.

If $FWHM \cdot \cos\theta$ vs. $\sin\theta$ plots (the Williamson-Hall plots) are drawn for the corresponding diffraction patterns obtained in case of investigated NM or UFG materials, then the microstrain can be estimated from the slope of variation and the crystallite size from the intercept with the vertical axis.

The properties of NM and UFG materials are superior to those of corresponding conventional coarse grained materials, the mechanical, microstructural and also physical characteristics being significantly improved through the advanced grain refinement [5]. For converting a coarse grained material into an UFG or nanostructured material, it is necessary both to impose an exceptionally high strain in order to introduce a high density of dislocations and for these dislocations to subsequently rearrange in order to form an array of grain boundaries [6-9]. A special set of techniques for the production of bulk nanostructured and UFG materials is based on severe plastic deformation (SPD), formally defined as those metal forming procedures in which a very high strain is imposed on a bulk solid without the introduction of any significant change in the overall dimensions of the solid. As a consequence, an exceptional grain refinement, is obtained with grain sizes mostly in the submicrometer or in the nanometer range [7].

From the variety of SPD procedures, equal channel angular pressing (ECAP) is the most interesting technique, because it can be applied to large specimens, so that there is the potential for producing UFG/NM that may subsequently be used in a wide range of structural applications. Also the potential for scaling up and developing ECAP at industrial level, is created for use in commercial metal processing procedures. ECAP can be applied to commercial pure metals and metal alloys, with face centered cubic, body centred cubic and hexagonal close packed crystal structures and coarse grains, to fabricate UFG/NM with no porosity and superior mechanical properties compared to the unprocessed material [10-13]. ECAP processing involves the passage of the sample (usually round or squared) through a die containing two intersecting channels identical in cross-section. As shown in figure 1*a*, the intersection angle is ϕ and a secondary angle of ψ sets the curvature from the outward intersection point of the channels [14-16].

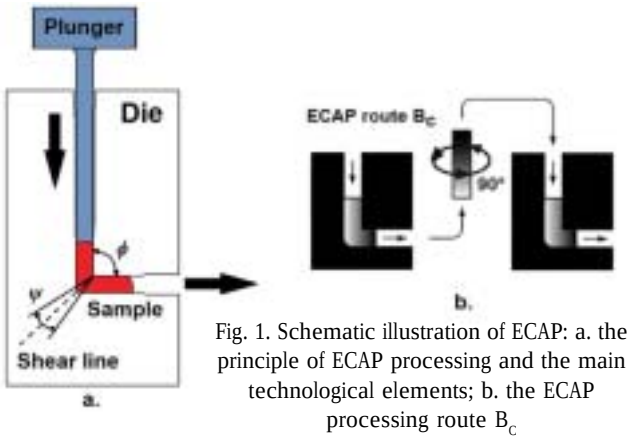

Fig. 1. Schematic illustration of ECAP: a. the principle of ECAP processing and the main technological elements; b. the ECAP processing route B_C

* *email: mihaibutu@yahoo.com; Tel.: 0747033884*

The sample moves like a rigid body, the deformation being performed quasi-ideally by simple shear in a thin layer (a plane) at the intersection of the two channels of the die (the shear plane) [17]. Despite the introduction of a very intense strain the sample ultimately emerges from the die without experiencing any change in the cross sectional dimensions. Since the cross sectional area remains unchanged, the same specimen may be pressed repetitively in order to attain exceptionally high strains and an advanced microstructure refinement [18]. Depending on the sample rotation, different processing routes denoted as (A, B_A, B_C and C) can be applied. Route A has no rotation of the sample, route B_A is rotated counter clockwise 90° on even number of passes and clockwise 90° on odd number of passes, route B_C is rotated counter clockwise 90° after every pass (fig. 1b) and route C is rotated 180° after every pass [19-23]. In our study, the ECAP processing route B_C was used, since it was found that the most promising experimental results are obtained when this route is applied [7, 9, 24, 25].

Al-Mg-Si alloys, like 6063 series, are some of the most widely used materials today which spans the entire range of industries. They are used in many consumer products, including pipes, railings, furniture, architectural extrusions, irrigation pipes and transportation. They are considered to be vital materials for nowadays society, being preferred mainly because they are leading to the reduction of the product weight. Aluminum was constantly highly demanded since the vast majority of its alloys are age hardenable and easily processable [26-29].

In our study, we examined a 6063 alloy, in the T1 condition, which is generally known as an architectural alloy. Mostly used for complex extrusions, 6063 aluminum alloy features a high corrosion resistance, a good surface finish and has a medium strength. Also, this alloy can be subjected to anodization and is well suited for welding. Consequently, the 6063 Al alloy is widely used for structural applications, in constructions, in transportation, for extreme sports equipment etc. Therefore, comprehending his behavior under various experimental conditions (strain rates, loadings, temperatures etc.) becomes a crucial problem.

Experimental part

The chemical composition for all investigated samples was determined by using a GNR *metal*-LAB 75/80V optical emission spectrometer (OES). The investigated material was originated from a 120 mm round extrusion billet stock, industrially manufactured using a continuous casting and heat treating technology. A METKON Servocut M300 abrasive cutter was used in order to obtain 60 x 9.6 x 9.6 mm initial dimensions for the ECAP samples. Cutting was done in such a manner that the sample and the billet axis are perpendicular. The ECAP processing die [30] had an intersection angle of $\phi = 90°$ and a secondary angle, ψ, of around 20°. As lubricant, graphite powder was used. By using a 200 ton-force hydraulic press, the specimens were processed at room temperature for one, three, six and nine ECAP passes respectively, at a pressing speed of 10 mm/s. The sample rotation was conducted following the SPD/ECAP deformation route B_C, preserving the same direction after each passage through the die (as shown in fig. 1b). The accumulated equivalent strain values ε_N were calculated using the die channel and relief angles in equation (2) [31]:

$$\varepsilon_N = N \cdot \frac{1}{\sqrt{3}}\left[2\operatorname{ctg}\left(\frac{\phi}{2}+\frac{\psi}{2}\right)+\psi\operatorname{csc}\left(\frac{\phi}{2}+\frac{\psi}{2}\right)\right] \quad (2)$$

where N is the number of passes, ϕ is the intersection angle and ψ is the corner angle.

According to equation (2) the equivalent strain depends on both ϕ and ψ angles. It decreases when ψ increases and the maximum ($\varepsilon_N \sim 1.15$) is obtained for $\phi = 90°$ and ψ close to zero. Equation (2) is an analytical expression for calculating the equivalent strain imposed after each ECAP passage only in terms of die geometric parameters.

Samples taken from all specimens (as-received and ECAP processed 6063-T1 aluminum alloy) were investigated in XRD tests for phase identification and Williamson-Hall analysis (evaluation of crystalline sizes and lattice strain). A precision cutter METKON Micracut 200 was used for obtaining 9 x 7 x 5 mm samples from each specimen, which were later hot mounted on a BUEHLER Simplimet 1000 automatic mounting press, each of them being subjected to grinding and polishing on a semiautomatic machine BUEHLER Phoenix 4000 Beta/1 Single. A PANalytical X'Pert PRO MPD diffraction system with copper anode ($K_{\alpha 1}$ = 1.54065 Å), gonio geometry and proportional detector was used for all the XRD measurements. The acquired raw data was processed in Crystal Impact Match! using ICDD PDF-2 database and fitted in PeakFit.

Results and discussions

The chemical composition, determined via OES and expressed as wt.%, for the 6063 aluminum alloy used in our experiments was: Si 0.458, Mg 0.616, Fe 0.326, Cu 0.091, Mn 0.089, Zn 0.074, Ti 0.014, Pb 0.013, Ni 0.002, Cr 0.010 and remainder Al.

Using equation (2) the accumulated equivalent strain was calculated for one, three, six and nine ECAP processing passes. The corner angle $\psi \sim 20°$, the intersection angle $\phi = 90°$, so the equivalent strain for each passage subjected to each specimen is approximately 1.05; therefore, the accumulated equivalent strain values are 1.05, 3.14, 6.33 and 9.49 respectively. Figure 2 shows that the variation of accumulated equivalent strain is linear dependent to the number of passes, the slop of variation being a function of ECAP die geometry, defined by the intersection angle and by the corner angle. The assumptions of this geometric analysis include simple shear, a frictionless die surface, a uniform plastic flow on a plane, a complete filling of the die channel by the billet and a rigid perfectly plastic material (no strain hardening behaviour is included). With these assumptions, equation (2) does not take into account for the effect of friction, strain hardening, strain distribution and deformation gradient, providing a homogeneous value of strain in the whole sample.

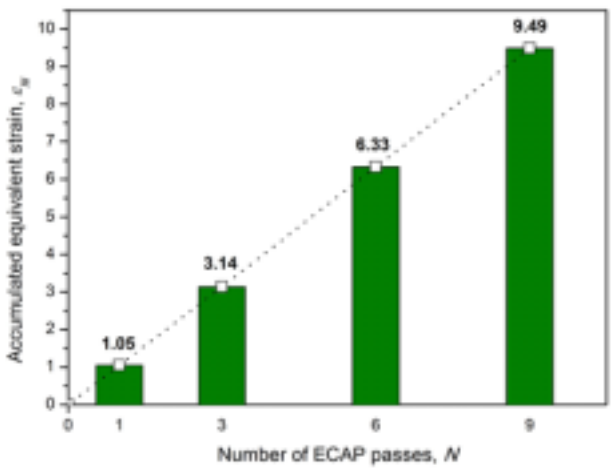

Fig. 2. Accumulated equivalent strain evolution as a function of ECAP pass number

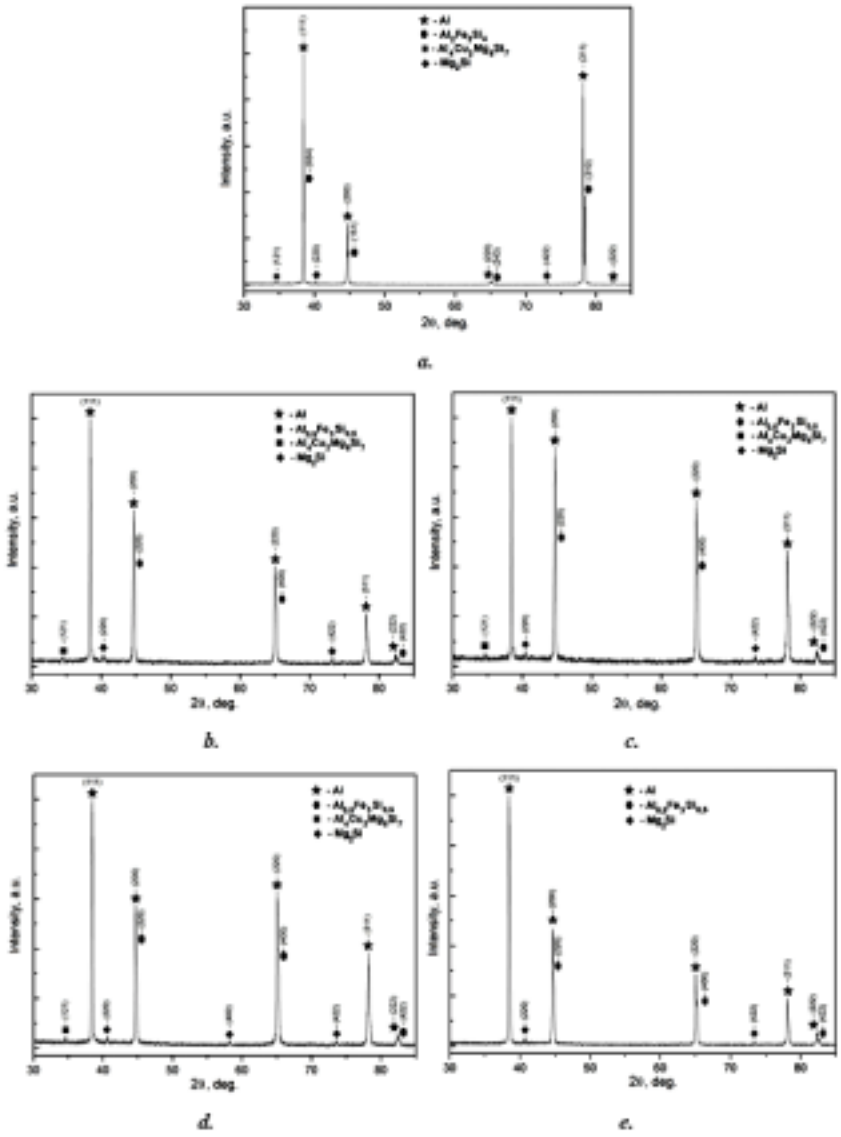

Fig. 3. X-Ray diffraction patterns of investigated 6063-T1 aluminum alloy: a. as-received (ε_N = 0.00); b. one ECAP pass (ε_N = 1.05); c. three ECAP passes (ε_N = 3.14); d. six ECAP passes (ε_N = 6.33); e. nine ECAP passes (ε_N = 9.49)

All samples (as-received and ECAP processed) were subjected to XRD analysis for phase identification. The achieved diffraction patterns, showing the variation of the X-Ray intensity versus the diffraction angle 2θ, are given in figure 3, the acquired raw data being processed in Crystal Impact Match! using ICDD PDF-2 database. Figure 3 shows the compounds that were indexed and therefore, the phases identified for these XRD records, namely: Al, $Al_2Fe_3Si_4$, $Al_4Cu_2Mg_8Si_7$, Mg_2Si for the as-received material; Al, $Al_{0.5}Fe_3Si_{0.5}$, $Al_4Cu_2Mg_8Si_7$, Mg_2Si for one, three and six passes ECAP processed material and Al, $Al_{0.5}Fe_3Si_{0.5}$, Mg_2Si for nine passes ECAP processed 6063 aluminum alloy, respectively. The $Al_4Cu_2Mg_8Si_7$ compound was no longer indexed for the maximum number of ECAP passes, mainly due to the severe fragmentation of secondary phase, generated by the high value of accumulated equivalent strain, correlated with this phase low ratio in the analyzed material. Also, one can observe that ECAP processing is leading to the stress induced transformation of the initial α-AlFeSi phase, the $Al_2Fe_3Si_4$ compound from the as-received material being indexed as $Al_{0.5}Fe_3Si_{0.5}$ in the processed alloy, regardless of the accumulated equivalent strain value and the number of ECAP passes.

As one can see in figure 3, the changes in diffraction peaks intensity are showing the preferential crystal orientation during ECAP processing, which is mainly driven by the shear plane interactions with the crystalline structure and the deformation texture and by the sample rotation system (the ECAP processing route) as well. Also, from figure 3, one can observe that the obtained diffraction peaks are wider for the ECAP processed material, suggesting a smaller dimension of crystallites, as compared to the as-received state, as a consequence of the advanced grain refinement obtained through ECAP processing.

By analyzing the XRD patterns for ECAP processed 6063-T1 aluminum alloy, crystallite size and microstrain can be evaluated using the Williamson-Hall (WH) technique. For plotting the WH diagrams, the achieved XRD patterns were initially fitted in PeakFit (only the first four high intensity Al diffraction peaks) and the crystalline domains were considered as being relatively spherical. Figure 4 illustrates both patterns (experimental and fitted) in case of one pass ECAP processed 6063-T1 alloy.

If the Williamson-Hall plots ($FWHM \cdot \cos\theta$ versus $\sin\theta$) are drawn for the obtained diffraction (XRD) patterns, according to equation (1), then the microstrain (the lattice strain) can be estimated from the slope of straight line and the crystallite size from the intercept with the vertical axis, as shown in figure 5.

After processing the WH plots (presented in fig. 5), the crystallite size was calculated as ranging from 37 nm, for one ECAP pass, to a minimum of 13 nm after nine ECAP processing steps (going through 26 nm for three passes and 14 nm for six passes). For the microstrain, the following values were determined: 3.19% for one ECAP pass, 3.81% for three passes, 4.07% for six passes and 3.08% for nine ECAP passes, respectively. The data obtained from the WH plots are shown in figure 6, where the crystallite size and

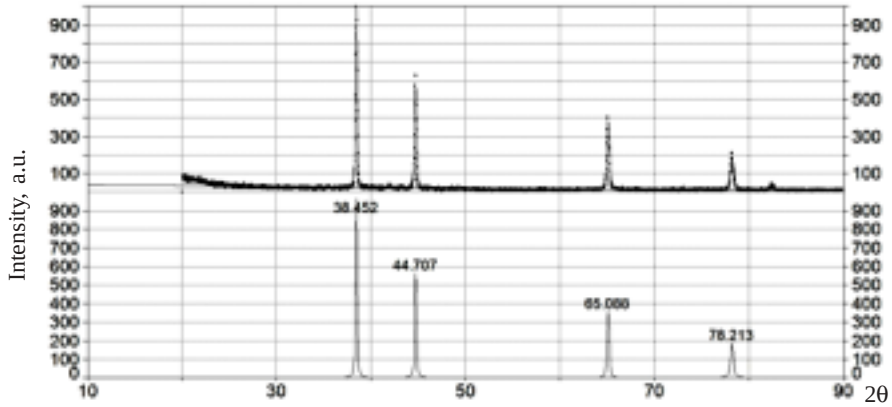

Fig. 4. X-Ray diffraction patterns of one pass ECAP processed 6063-T1 alloy: experimental (up) and fitted in PeakFit (down)

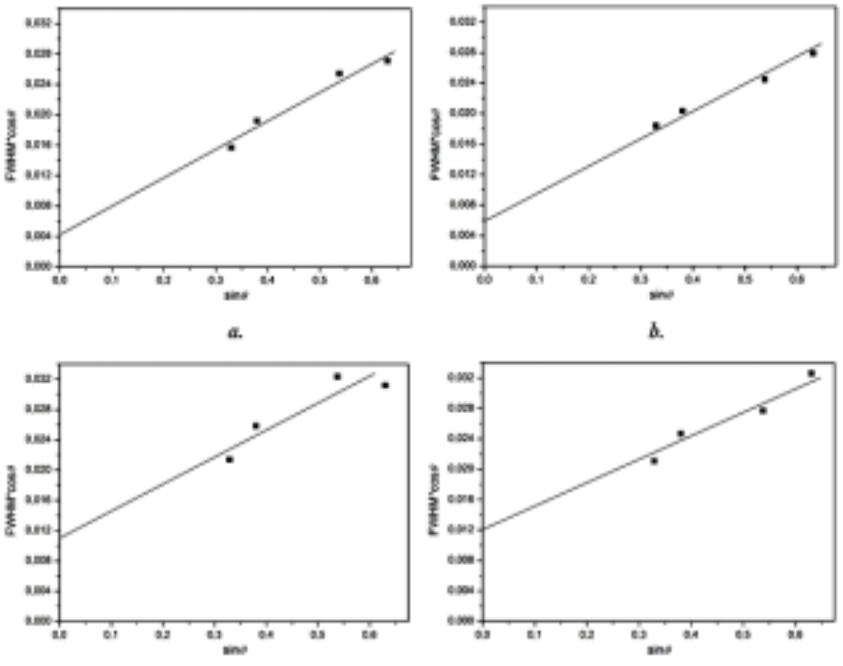

Fig. 5. Williamson-Hall plots for SPD/ECAP processed 6063-T1 aluminum alloy: a. one ECAP pass (ε_N = 1.05); b. three ECAP passes (ε_N = 3.14); c. six ECAP passes (ε_N = 6.33); d. nine ECAP passes (ε_N = 9.49)

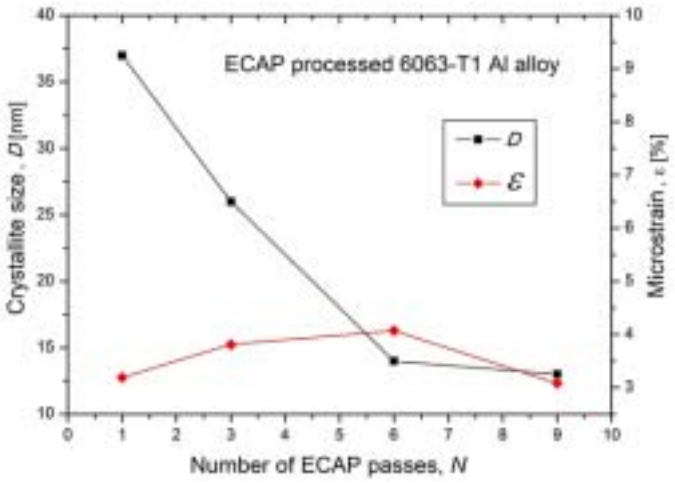

Fig. 6. Crystallite size and microstrain evolution versus the number of ECAP passes for the investigated 6063-T1 aluminum alloy

the microstrain are represented as a function of accumulated equivalent strain (the number of ECAP passes).

By analyzing the data presented in figure 6, one can observe that the microstructural refinement of 6063-T1 Al alloy is relatively intense in the first stage of the process, for up to six ECAP passages through the die (the crystallite size decreasing from 37 nm for the first ECAP pass, to 14 nm after six passes). Increasing the number of ECAP passes furthermore (up to nine) results only in an insignificant crystallite size reduction (up to 13 nm).

Regarding the microstrain, one can observe an increasing from 3.19% for the first pass, up to nearly 4.1% after six ECAP passages through the die. Further increasing the number of passes (the accumulated equivalent strain), results in a reduction of microstrain, this parameter reaching a value of approximately 3.1% after nine ECAP processing steps. Also, should be noted that the lattice strain is relatively high for all the ECAP processed specimens, most likely due to the high values of the equivalent strain imposed in each ECAP pass. Thus, we can say that the grain refining process reaches saturation after six ECAP passages through the 90° die, further SPD processing leading only to a decrease of the microstrain.

In order to explain the observed behavior, a shift in the deformation mechanism at a certain nanometer level should be considered. This phenomenon was observed by other researchers [32] as well, being described as a new plastic deformation mechanism, considerably different from that of normal metallic materials. Even though this is difficult to be proved, it is considered that the deformation progresses by giant faults development, crystal lattice local disturbances at nanometer scale being possible, and generating localized strain fields.

Conclusions

In our present study, we evaluated the crystallite size and lattice strain (microstrain) evolution as a function of accumulated equivalent strain (the number of passages

through the die) in a nanostructured 6063-T1 aluminum alloy severely deformed by ECAP. Chemical composition for the investigated material was initially determined in OES experiments and the accumulated equivalent strain was estimated based on ECAP die geometric parameters and on the number of passes. It was found that the variation of accumulated equivalent strain is linear dependent to the number of passes, the slope of variation being a function of ECAP die geometry, defined by the channel intersection angle and by the corner angle. An in-depth XRD analysis was performed for phase identification and crystallite size and microstrain estimation using the Williamson-Hall technique. The phases identified for the investigated material were Al, AlFeSi, AlCuMgSi and Mg_2Si, being found that ECAP processing is leading to the stress induced transformation of the initial α-AlFeSi phase, the $Al_2Fe_3Si_4$ compound found in the unprocessed material being indexed as $Al_{0.5}Fe_3Si_{0.5}$ in all ECAP processed samples. The Williamson-Hall analysis showed the advanced microstructural refinement obtained by ECAP processing. The crystallite size decreased intensely and the microstrain increased in the first stages of SPD/ECAP process, for up to six passes. Further increasing the number of passes (the accumulated equivalent strain) up to nine, leads only to a reduction of the microstrain, the decrease of crystallite size decreasing being insignificant. Therefore, we can conclude that in the 6063-T1 aluminum alloy, severely deformed by ECAP, the microstructural refinement process reaches saturation after six passes, further SPD processing leading only to the decreasing of the lattice strain, the crystallite size nearly unvarying after six processing steps.

Acknowledgements: This work has been funded by the Sectoral Operational Programme Human Resources Development 2007-2013 of the Ministry of European Funds through the Financial Agreement POSDRU/159/1.5/S/134398.

References

1.R. Z. VALIEV, Y. ESTRIN, Z. HORITA, T. G. LANGDON, M. J. ZEHETBAUER, Y. T. ZHU, JOM, **58**, 2006, p. 33.
2.Y. BEYGELZIMER, V. VARYUKHIN, D. ORLOV, B. EFROS, V. STOLYAROV, H. SALIMGAREYEV, Ultrafine Grained Materials II, TMS, Warrendale PA, 2002.
3. M. J. ZEHETBAUER, R. Z. VALIEV, Nanomaterials by Severe Plastic Deformation, Wiley-VCH, Weinheim, 2004.
4. U. HOLZWARTH, N. GIBSON, Nat. Nanotechnol., **6**, no. 9, 2011, p. 534.
5. V. D. COJOCARU, D. RADUCANU, N. SERBAN, I. CINCA, R. SABAN, U.P.B. Sci. Bull. B, **72**, no. 3, 2010, p. 193.
6. R. Z. VALIEV, R. K. ISLAMGALIEV, I. V. ALEXANDROV, Prog. Mater. Sci., **45**, 2000, p. 103.
7. R. Z. VALIEV, T. G. LANGDON, Prog. Mater. Sci., **51**, 2006, p. 881.
8. N. SERBAN, N. GHIBAN, V. D. COJOCARU, JOM, **65**, 2013, p. 1411.
9. N. SERBAN, V. D. COJOCARU, M. BUÞU, JOM, **64**, 2012, p. 607.
10. V. V. STOLYAROV, Y. T. ZHU, T. C. LOWE, R. Z. VALIEV, Mater. Sci. Eng. A, **303**, 2001, p. 82.
11. M. MUKAI, M. YAMANOI, H. WATANABE, K. HIGASHI, Scripta Mater., **45**, 2001, p. 89.
12. W. J. KIM, C. W. AN, Y. S. KIM, S. I. HONG, Scripta Mater., **47**, 2002, p. 39.
13. W. J. KIM, J. K. KIM, Y. T. PARK, S. I. HONG, I. D. KIM, Y. S. KIM, J. D. LEE, Metall. Mater. Trans. A, **33**, 2002, p. 3155.
14. N. SERBAN, V. D. COJOCARU, M. BUTU, U.P.B. Sci. Bull. B., **73**, no. 4, 2011, p. 213.
15. N. SERBAN, V. D. COJOCARU, D. RĂDUCANU, M. BUTU, R. SABAN, E. IBRAIM, U.P.B. Sci. Bull. B., **73**, no. 3, 2011, p. 237.
16. N. SERBAN, D. RADUCANU, V. D. COJOCARU, N. GHIBAN, Adv. Mat. Res., **1114**, 2015, p. 143.
17. K. NAKASHIMA, Z. HORITA, M. NEMOTO, T. G. LANGDON, Mater. Sci. Eng. A, **281**, 2000, p. 82.
18. V. M. SEGAL, Mater. Sci. Eng. A, **197**, 1995, p. 157.
19. M. FURUKAWA, Y. IWAHASHI, Z. HORITA, M. NEMOTO, T. G. LANGDON, Mater. Sci. Eng. A, **257**, 1998, p. 328.
20. S. L. SEMIATIN, D. P. DELO, E. B. SHELL, Acta Mater., **48**, 2000, p. 1841.
21. L. DUPUY, J. J. BLANDIN, Acta Mater., **50**, 2002, p. 3251.
22. L. OLEJNIK, A. ROSOCHOWSKI, B., Bull. Pol. Acad. Sci. Tech.. Sci., **53**, 2005, p. 413.
23. S. FERRASSE, V. M. SEGAL, F. ALFORD, J. KARDOKUS, S. STROTHERS, Mater. Sci. Eng. A, **493**, 2008, p. 130.
24. J. ZRNIK, S. V. DOBATKIN, I. MAMUZIC, Metalurgija, **47**, 2008, p. 211.
25. Z. HORITA, M. FURUKAWA, M. NEMOTO, T. G. LANGDON, Mater. Sci. Tech., **16**, 2000, p. 1239.
26. MINEA, A.A., SANDU, I.G., Mat. Plast., **44**, no. 4, 2007, p. 370.
27. R. Z. VALIEV, D. A. SALIMONENKO, N. K. TSENEV, P. B. BERBON, T. G. LANGDON, Scripta Mater., **37**, 1997, p. 1945.
28.M. AI-BIN, Y. NISHIDA, J. JING-HUA, N. SAITO, I. SHIGEMATSU, A. WATAZU, Trans. Nonferrous Met. Soc. China, **17**, 2007, p. 104.
29. TACHE, F., STOICA,A., STROESCU,M., DOBRE, T., Mat. Plast., **47**, no. 1, 2010, p. 16.
30. N. SERBAN, D. RĂDUCANU, V. D. COJOCARU, A. GHIBAN, Adv. Mat. Res., **1114**, 2015, p. 129.
31.Y. IWAHASHI, Z. HORITA, M. NEMOTO, T. G. LANGDON, Acta Mater., **45**, no. 11, 1997, p. 4733.
32. T. SAITO, T. FURUTA, J. H. HWANG, Science, **300**, 2003, p. 464

Manuscript received: 5.10.2015

Reinnoiti-va abonamentele
la REVISTA DE CHIMIE si
revista MATERIALE PLASTICE
pe anul 2016

Pretul unui abonament la
REVISTA DE CHIMIE este de:
200 lei pentru persoana fizica
400 lei pentru universitati
500 lei pentru societati comerciale

si la revista

MATERIALE PLASTICE este de:
150 lei pentru persoanã fizica
200 lei pentru universitati
300 lei pentru societati comerciale
Conturi:
S.C. BIBLIOTECA CHIMIEI SA

RO20 RNCB 0072049700600001 BCR sector 1
RO51 TREZ 7065069XXX002561 Trez. sect. 6

C.U.I. RO 13751581